JOURNAL OF GEOPHYSICAL RESEARCH: BIOGEOSCIENCES, VOL. 118, 1593–1603, doi:10.1002/2013JG002495, 2013

Nocturnal soil CO_2 uptake and its relationship to subsurface soil and ecosystem carbon fluxes in a Chihuahuan Desert shrubland

Erik P. Hamerlynck,[1] Russell L. Scott,[1] Enrique P. Sánchez-Cañete,[2,3] and Greg A. Barron-Gafford[4]

Received 26 August 2013; revised 24 October 2013; accepted 26 October 2013; published 6 December 2013.

[1] Despite their prevalence, little attention has been given to quantifying arid land soil and ecosystem carbon fluxes over prolonged, annually occurring dry periods. We measured soil [CO_2] profiles and fluxes (F_s) along with volumetric soil moisture and temperature in bare interplant canopy soils and in soils under plant canopies over a three-month hot and dry period in a Chihuahuan Desert shrubland. Nocturnal F_s was frequently negative (from the atmosphere into the soil), a form of inorganic carbon exchange infrequently observed in other deserts. Negative F_s depended on air-soil temperature gradients and were more frequent and stronger in intercanopy soils. Daily integrated ecosystem-level F_s was always positive despite lower daily F_s in intercanopy soils due to nocturnal uptake and more limited positive response to isolated rains. Subsurface [CO_2] profiles associated with negative F_s indicated that sustained carbonate dissolution lowered shallow-soil [CO_2] below atmospheric levels. In the morning, positive surface F_s started earlier and increased faster than shallow-soil F_s, which was bidirectional, with upward flux toward the surface and downward flux into deeper soils. These dynamics are consistent with carbonate precipitation in conjunction with convection-assisted CO_2 outgassing from warming air and soil temperatures and produced a pronounced diurnal F_s temperature hysteresis. We concluded that abiotic nocturnal soil CO_2 uptake, through a small carbon sink, modulates dry season ecosystem-level carbon dynamics. Moreover, these abiotic carbon dynamics may be affected by future higher atmospheric carbon dioxide levels and predictions of more prolonged and regular hot and dry periods.

Citation: Hamerlynck, E. P., R. L. Scott, E. P. Sánchez-Cañete, and G. A. Barron-Gafford (2013), Nocturnal soil CO_2 uptake and its relationship to subsurface soil and ecosystem carbon fluxes in a Chihuahuan Desert shrubland, *J. Geophys. Res. Biogeosci.*, *118*, 1593–1603, doi:10.1002/2013JG002495.

1. Introduction

[2] Southwestern North American climate conditions are predicted to become increasingly arid, with disproportionate decreases in winter time rainfall and greater variation in summer rains associated with the North American monsoon [*Seager et al.*, 2007; *McAfee and Russell*, 2008]. Reduced cool season rains and more variation in the timing and total amount of monsoon season rains will likely increase the duration and severity of the "premonsoon drought," a period of typically low rainfall that occurs from April to mid-June [*Sheppard et al.*, 2002; *McAfee and Russell*, 2008]. The premonsoon drought represents a consistent annual challenge for long-lived perennial plants in the arid southwest U.S. and, hence, the stability and structure of its water-limited ecosystems. Recent wide-spread regional mortality of dominant species across arid and semiarid southwest U.S. ecosystems has been closely associated with multiple dry years with low winter precipitation [*Breshears et al.*, 2005; *Miriti et al.*, 2007; *McAuliffe and Hamerlynck*, 2010], and such mortality events can strongly modulate ecosystem processes and productivity responses to subsequent monsoon season rain [*Pennington and Collins*, 2007; *Scott et al.*, 2010; *Hamerlynck et al.*, 2013]. Ecological processes in arid land systems are highly "pulsed" and are tightly coupled to the seasonal distribution as well as the total amount of individual rainfall events [*Loik et al.*, 2004]. Due to this, much arid land ecosystem flux research has focused on transitions to and from periods of low and high moisture availability [*Huxman et al.*, 2004; *Potts et al.*, 2006; *Cable et al.*, 2008; *Jenerette et al.*, 2008; *Serrano-Ortiz et al.*,

[1]USDA-ARS Southwest Watershed Research Center, Tucson, Arizona, USA.
[2]Estación Experimental de Zonas Áridas, Consejo Superior de Investigaciones Científicas, Almería, Spain.
[3]Centro Andaluz de Medio Ambiente, Granada, Spain.
[4]School of Geography and Development and B2 Earthscience, University of Arizona, Tucson, Arizona, USA.

Corresponding author: E. Hamerlynck, USDA-ARS Southwest Watershed Research Center, 2000 E. Allen Rd., Tucson, AZ 85719, USA. (erik.hamerlynck@ars.usda.gov)

2169-8953/13/10.1002/2013JG002495

2010; *Barron-Gafford et al*., 2012; *Rey et al*., 2012; *Yates et al*., 2013], rather than over prolonged and predictable seasonal dry periods, which are a defining characteristic of arid land ecosystems [*Loik et al*., 2004].

[3] A fundamental shift in ecosystem processes could potentially occur under prolonged dry periods. There is increasing evidence that abiotic carbon dynamics affect arid land ecosystem-level gas exchange over prolonged, dry plant dormant periods [*Emmerich*, 2003; *Kowalski et al*., 2008; *Serrano-Ortiz et al*., 2010; *Plestenjak et al*., 2012; *Rey et al*., 2012; *Roland et al*., 2013; *Sánchez-Cañete et al*., 2013a]. Recently, *Roland et al*. [2013] have used a chemical carbonate weathering model to demonstrate how turbulence-induced ventilation drives soil CO_2 outgassing and carbonate precipitation during the day, while nocturnal replenishment of soil CO_2 and dissolution of carbonates can drive soil CO_2 uptake over dry periods in Spanish mattoral. Observations of negative nocturnal soil efflux (F_s), or soil uptake of CO_2 from the atmosphere, have been found in other arid land systems, notably the dry valley ecosystems of Antarctica [*Parsons et al*., 2004; *Ball et al*., 2009] and in highly alkaline soils of the Gubantonggut Desert in China [*Xie et al*., 2009] have been primarily attributed to physical, not biological, processes. Negative F_s has been found to depend on changes in strength of soil temperature gradients and soil electrical conductivity and are usually most pronounced under low soil water contents [*Ball et al*., 2009; *Xie et al*., 2009]. Deserts frequently have strong soil temperature gradients that contribute to abiotic and plant-mediated soil moisture distribution and soil respiration [*Nobel and Geller*, 1987; *Williams et al*., 1993; *Scanlon*, 1994; *Berndtsson et al*., 1996; *Fernandez et al*., 2006; *Scott et al*., 2008; *Barron-Gafford et al*., 2011]. These dry, hot conditions are typical of the annual premonsoon drought and could induce prolonged negative surface F_s. Soil carbon flux is a critical determinant of arid land net ecosystem carbon dioxide exchange (NEE) and modulates ecosystem carbon sink or source potential [*Cable et al*., 2011; *Hamerlynck et al*., 2013]. Even if nighttime soil CO_2 uptake rates are small, quantification of such dynamics would contribute to a fuller understanding of arid land ecosystem carbon balance [*Ball et al*., 2009; *Serrano-Ortiz et al*., 2010]. However, past research examining negative F_s has not been coupled directly with concurrent measurements of subsurface [CO_2], nor has the spatially explicit sampling been performed needed to extrapolate this phenomenon to ecosystem-level F_s [*Barron-Gafford et al*., 2011]. Thus, the importance of negative F_s and its relationship to ecosystem-level fluxes in any terrestrial arid land ecosystem is currently unknown.

[4] Arid land systems are shifting mosaics of undercanopy and bare soil intercanopy space [*Scholes and Archer*, 1997; *D'Odorico et al*., 2007]. Woody shrubs serve as important foci for biological activity, as they facilitate accumulation of limiting nutrient resources [*Titus et al*., 2002] and ameliorate high temperature and radiation loads which can, in some cases, enhance plant soil water availability [*Bhark and Small*, 2003; *D'Odorico et al*., 2007, 2010; *Pockman and Small* 2010; but see *Caldwell et al*., 2008; *Duniway et al*., 2010]. Soil fluxes are almost always higher under semiarid and arid land plant canopies, which are typically associated with higher biotic activity [*Cable et al*., 2008; *Barron-Gafford et al*., 2011; but see *Bowling et al*., 2011]. Strong soil temperature gradients commonly cooccur with negative surface F_s [*Ball et al*., 2009; *Parsons et al*., 2004; *Xie et al*., 2009], and such gradients may be reduced in strength under plant canopies [*D'Odorico et al*., 2010]. The higher probability of biological activity under plant canopies [*Barron-Gafford et al*., 2011] may also limit the frequency and strength of negative soil F_s. In addition, soil contributions are likely the dominant contribution to ecosystem respiration (R_{eco}) across plant dormant spring and autumn periods [*Emmerich*, 2003]. If nocturnal surface F_s is consistently higher and positive in undercanopy locations across premonsoon drought periods, disproportionate contributions from undercanopy soils may sustain positive ecosystem-scale soil fluxes [*Barron-Gafford et al*., 2011]. Thus, plant canopies likely modulate the spatial and temporal dynamics of soil carbon dioxide fluxes in arid land systems over prolonged seasonal dry periods.

[5] Here we present a study aimed at quantifying soil respiration and soil surface and subsurface CO_2 dynamics of a Chihuahuan Desert shrubland across a three-month premonsoon drought period. The three main objectives of this study were as follows:

[6] 1. To quantify the frequency, strength, and spatial occurrence of negative F_s. Specifically, we hypothesized that negative F_s would be more likely and of greater magnitude in intercanopy locations, as these are more likely to have the strong temperature gradients associated with negative F_s [*Ball et al*., 2009; *Xie et al*., 2009].

[7] 2. To determine where and when negative F_s affect ecosystem-level soil F_s dynamics. We hypothesized that the flux rates associated with negative F_s [*Parsons et al*., 2004; *Ball et al*., 2009; *Xie et al*., 2009] are too low to result in negative F_s when integrated over 24 h or of sufficient magnitude in intercanopy soils to offset positive undercanopy F_s to induce negative ecosystem-level nighttime soil efflux.

[8] 3. To establish the temporal relationship between surface F_s and subsurface CO_2 gas concentration gradients and associated CO_2 flux. Previous studies demonstrating nighttime NEE or soil CO_2 uptake did not measure covariation of surface F_s with subsurface CO_2 [*Ball et al*., 2009; *Xie et al*., 2009; *Roland et al*., 2013]. Comeasurement of surface and subsurface CO_2 dynamics will provide resolution of where in the soil profile negative F_s originates. We hypothesized that subsurface changes in [CO_2] would precede surface CO_2 uptake.

2. Materials and Methods

2.1. Study Site

[9] The study was conducted at the Lucky Hills site located within in the U.S. Department of Agriculture (USDA) Agricultural Research Service Walnut Gulch Experimental Watershed located near Tombstone, AZ, USA. The Lucky Hills site is located around 31.744°N and 110.052°W with an elevation of 1370 m. Lucky Hills is a typical Chihuahuan Desert shrub plant community dominated by creosote bush (*Larrea tridentata*), whitethorn acacia (*Acacia constricta*), mariola (*Parthenium incanum*), and tarbush (*Flourensia cernua*), with average woody plant canopy cover of 34% and bare soil cover of 66% [*Skirvin et al*., 2008]. The 1990–2009 mean annual precipitation at Lucky Hills was about 280 mm, with air temperatures ranging from a minimum of −5°C to a maximum of over 40°C [*Goodrich et al*., 2008, *Keefer et al*., 2008]. Approximately 60% of the

annual rainfall comes during the months of July–September in the form of convective thunderstorms associated with North American monsoon [*Sheppard et al*., 2002], with the bulk of the rest falling over the cooler nonsummer months [*Renard et al*., 2008]. Soils at the site are from the Lucky Hills series (coarse-loamy, mixed, thermic, Ustochreptic Calciorthids) with very gravelly sandy loam A horizons (0–7 cm) with relatively low $CaCO_3$ (9% fine fraction) and pH 8.2, followed by two loamy B horizons with varying degrees of carbonate accumulation (Bk horizons), the first from 7 to 32 cm (Bk1) with pH 8.6 and 35% $CaCO_3$ fine soil fraction and the second (Bk2; 32–52 cm) with pH 8.4 and 44% fine fraction $CaCO_3$, then a coarse sandy loam Bk horizon with a weakly cemented, discontinuous calcium carbonate ("caliche") layer (Bkm3; 55–72 cm), and a fine soil fraction with 33% $CaCO_3$ and pH 8.2 [*Breckenfeld*, 2008].

2.2. Meteorological Measurements

[10] We have measured hydrometeorological variables and carbon dioxide and water vapor fluxes using the eddy covariance (EC) technique at the Lucky Hills site continuously since 2007 [*Scott et al*., 2010]. The principal role of the EC station for this study was to provide meteorological data for calculating gradient-based subsurface soil CO_2 fluxes (see below) and to determine if soil/atmospheric temperature conditions were conducive to dew formation.

2.3. Soil Surface and Subsurface CO_2 Dynamics

2.3.1. Surface CO_2 Flux

[11] On 23 March 2012, we deployed a multichamber soil respiration monitoring system (LI-8100, LiCOR Instruments, Lincoln, NE) consisting of eight chambers, four placed under creosotebush (*Larrea tridentata*) and four in intercanopy spaces. Soil collars were inserted 8–9 cm into the soil surface, leaving 2–3 cm of the collar exposed; this exposed height was used to calculate the chamber volume needed to estimate soil CO_2 efflux (F_s in μmol m^{-2} s^{-1}). F_s was measured every 2 h by enclosing the chamber and measuring the CO_2 molar fraction [CO_2] every second over a 2 min measuring interval following a 45 s premeasurement purge. F_s were calculated from an exponential or a linear regression of [CO_2] on time after selecting the regression technique with the lowest number of iterations and the highest coefficient of determination (R^2; File Viewer v3.0, LiCOR Instruments). The nondispersive infrared gas analyzer in LiCOR 8100 has a published measurement range of 0–20,000 ppm, with reading accuracy of 1.5%, and a zero drift of <1 ppm d^{-1} and a total calibration drift of <0.4 ppm $°C^{-1}$ at 370 ppm, with RMS noise of <1 ppm with 1 s signal averaging. Concurrent with [CO_2] sampling, chamber air temperature (T_{air}) was measured with a thermistor attached to the chamber housing. Soil temperature (T_{soil}) was measured with a LiCOR temperature probe, and volumetric soil moisture (θ, cm^3 cm^{-3}) was measured with a Decagon ECH_2O 5 cm probe inserted horizontally at 15 cm depth into a trench face dug adjacent to the monitored soil plot and subsequently reburied. T_{air}, T_{soil}, and θ were averaged over each 2 min efflux measurement. Intercanopy and undercanopy plots were paired for concurrent sampling to insure that diel temperature effects were spread evenly across plot types. Nighttime average F_s was calculated from values obtained between 22:00 MST of the previous day and 06:00 of the current day of year (DOY). Daily integrated molar soil efflux was estimated by determining the area under each 24 h curve, with nighttime molar efflux estimated by determining the area under curves generated from 20:00 the night before to 06:00 MST of the current DOY (area transform function, SigmaPlot v10.0). Undercanopy and intercanopy integrated F_s carbon yields were extrapolated to ecosystem-level F_s by multiplying the mean of each F_s by their respective cover values of 34% and 66% [*Skirvin et al*., 2008].

2.3.2. Subsurface Soil CO_2 Concentrations and Flux

[12] Soil surface CO_2 concentrations were estimated from intercanopy soil respiration chambers every 2 h by averaging chamber [CO_2] over 10 s following the 45 s chamber prepurge before the chamber deployed over each of the soil efflux collars described above. Subsurface volumetric CO_2 fraction (ppm) was measured using CO_2 sensors equipped with solid-state compact CO_2 probes (GM222, Vaisala, Helsinki, Finland). We measured the volumetric soil CO_2 fractions across three intercanopy soil profiles, each consisting of three CO_2 sensors (with a range of 0–5000 μmol mol^{-1}) and soil temperature at 2, 8, and 16 cm, with soil moisture probes spanning the 2–8 and 8–16 cm measurement intervals. In addition, these parameters were measured at 20 and 40 cm at a single location located within 3 m of the three 2–16 cm profiles. Each probe was encased in a vertical PVC pipe with an open bottom that terminated at the desired depth in the soil, and this casing was sealed on the upper end using a rubber gasket that fits snugly between the probe and the pipe housing (in the sense of *Barron-Gafford et al*. [2011]). [CO_2] at each depth was sampled every 30 s, and 30 min averages were stored in the data logger. The [CO_2] readings were corrected for field variations in soil temperature and atmospheric pressure using the data collected by the eddy covariance tower [*Tang et al*., 2003]. To ensure accuracy, approximately every month, measured concentrations of each CO_2 probe were compared against the other two profile probes located at the same depth. When in situ concentrations differed by more than ±50 ppm, all three probes were pulled and exposed to open air. If all three probes differed by no more than ~30 ppm from atmospheric concentrations, differences were considered to be due to spatial variation and not probe malfunctioning or calibration drift. Otherwise, the questionable probe was replaced by a new probe that had been zeroed and span calibrated to 3000 ppm in the laboratory. Published probe accuracy is ±1.5% of the range, ±2% of the reading.

[13] Soil CO_2 efflux (F_s; μmol m^{-2} s^{-1}) from the profile was obtained using a computational approach based on Fick's law and accounting for gradient conservation–dependent mass diffusion of gasses [*Bird et al*., 2002; *Kowalski and Argüeso*, 2011], with $F_s = -D_s \rho_a (\delta C/\delta z)$, where D_s is the soil CO_2 diffusion coefficient (m^2 s^{-1}), ρ_a is the molar air density (μmol m^{-3}), and $\delta C/\delta z$ is the vertical CO_2 molar fraction gradient (ppm m^{-1}). D_s was calculated for each depth as $D_s = \xi D_a$, where ξ is the tortuosity factor, and D_a is the diffusion coefficient of CO_2 in free air. Tortuosity was calculated as $\xi = [(\phi - \theta)^{2.5}]/\phi$, where ϕ is porosity, calculated as $\phi = \rho_b/\rho_m$, with ρ_b as bulk density and ρ_m as the particle density of mineral soil (1.64 g cm^{-3} and 2.65 g cm^{-3} for the upper 15 cm of soil, respectively), and θ is the volumetric soil water content [*Moldrup et al*., 2000]. D_a (m^2 s^{-1}) was calculated as per *Jones* [1992], with $D_a = D_{a0}(P/101.3)^* (T/293.16)^{1.75}$, where D_{a0} is a reference value of D_a at 293 K

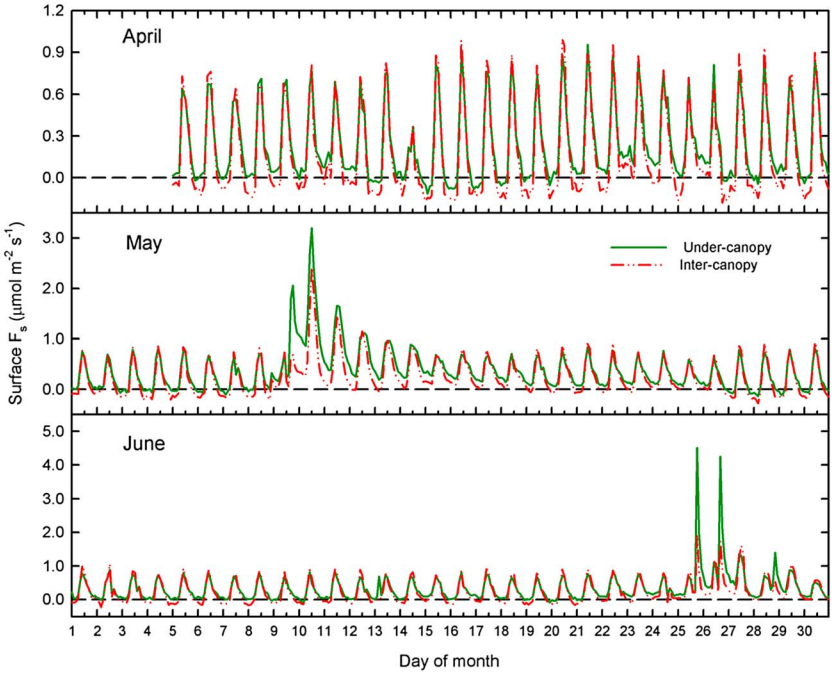

Figure 1. Three month time series of diurnal soil CO_2 efflux (F_s) measured in undercanopy (solid line) and intercanopy locations (broken line) in a Chihuahuan Desert shrubland during the 2012 premonsoon dry period. Measurements were made every 2 h, each line is the mean of measurements from four F_s collars; note differences in y axis scales; the dashed reference line indicates $F_s = 0$.

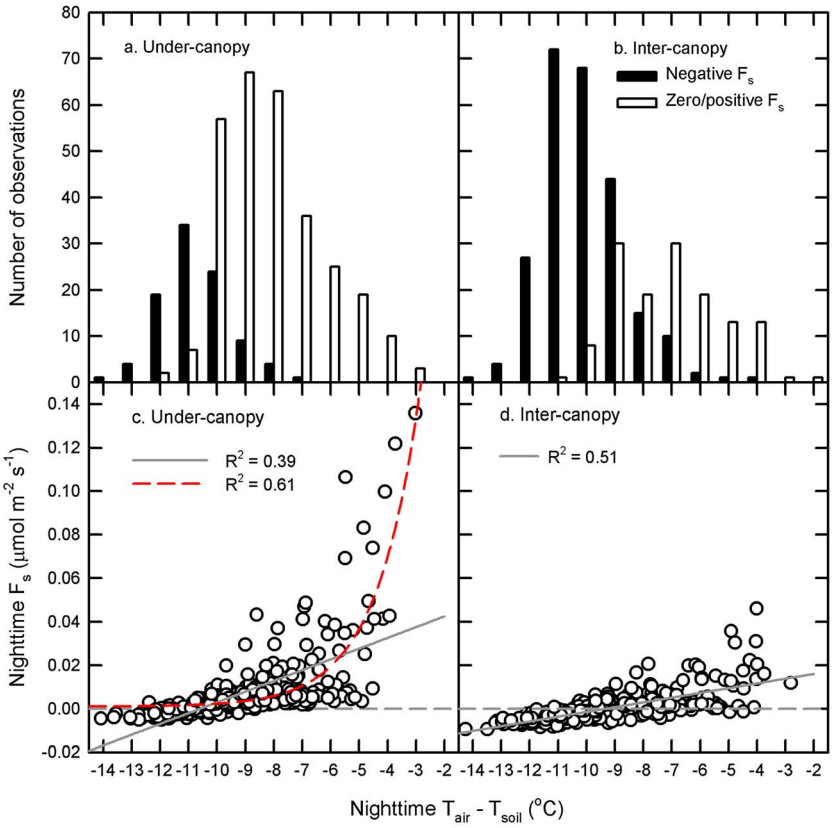

Figure 2. Frequency of negative and zero/positive nocturnal soil surface CO_2 efflux (F_s) observations for (a) undercanopy and (b) intercanopy soils. Regression relationships for nocturnal F_s with (c) undercanopy and (d) intercanopy air-soil temperature gradients. Negative temperature differences indicate that soils at 15 cm depth are warmer than air temperature; the dashed reference lines indicate $F_s = 0$.

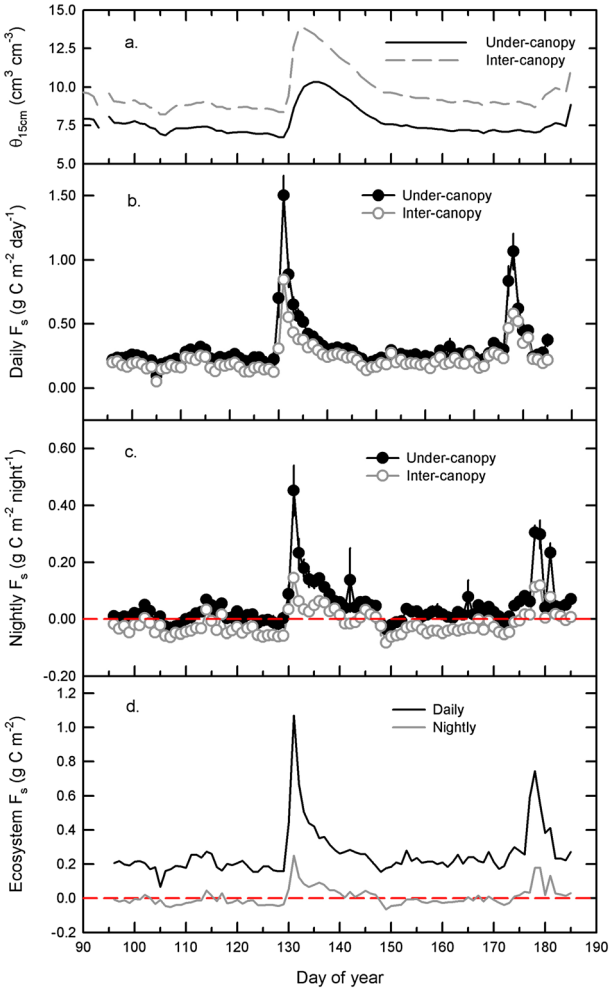

Figure 3. Intercanopy and undercanopy (a) daily average volumetric soil moisture, (b) 24 h and (c) nightly (20:00–06:00 MST) integrated soil efflux (F_s) carbon yield, and (d) ecosystem-level daily and nightly F_s carbon yields over the course of the 3 month 2012 premonsoon study period. Dashed lines are F_s zero references; each F_s point and $\theta_{15\ cm}$ line is the mean of four soil efflux collars; error bars are ±1 SE.

and 101.3 kPa ($D_{a0} = 1.47 \times 10^{-5}$ m^{-2} s^{-1}), P is air pressure (kPa), and T is temperature (K).

2.4. Statistical Analysis

[14] Negative and positive undercanopy and intercanopy F_s values were binned into 1°C chamber $T_{air} - T_{soil}$ differences, and the differences in F_s distributions across these temperature bins were compared using chi-square analysis (χ^2, Statistix v.8.0, Analytical Software, Tallahassee, FL). The dependence of nighttime F_s on the air-soil temperature gradient was determined by regressing instantaneous measures of F_s against concurrent chamber $T_{air} - T_{soil}$ and comparing the fitted slopes and intercepts (linear regression, Statistics v8.0). To determine if the magnitude of negative F_s differed between intercanopy and undercanopy locations, we performed a one-way analysis of variance (ANOVA) comparing nighttime F_s for those nights where both locations showed sustained negative F_s, using the location-by-replicate interaction as the ANOVA F test error term. To determine seasonal differences in undercanopy and intercanopy 24 h and nighttime-integrated F_s, we used a split-plot repeated-measures one-way analysis of variance (RM-ANOVA, Statistix v8.0). Soil efflux collar location (intercanopy and undercanopy) was used as the whole-plot effect, using the location-by-replicate collar ($n = 4$ for each location) as the whole-plot F test error term. Day of year (DOY) and the DOY-by-location interactions were the subplot, within-treatment effects, using the nested location-by-DOY-by-replicate interaction as the subplot F test error term. Of specific interest in this RM-ANOVA was the location-by-DOY interaction, as this would show location-specific differences in surface F_s to environmental variation over the three-month sampling period. Final intercanopy and undercanopy comparison was one-way ANOVA of F_s summed for all 24 h diel and nighttime intercanopy and undercanopy observations, using the location-by-replicate collar interaction as the ANOVA F test error term. For all one-way and RM-ANOVA, post hoc means testing was made using α-adjusted least significant difference ($P < 0.05$).

3. Results

[15] Across the three-month study period, negative surface F_s occurred in both collar locations (Figure 1) but was more frequent and occurred across a wider range of nighttime air-soil temperature differences in intercanopy compared

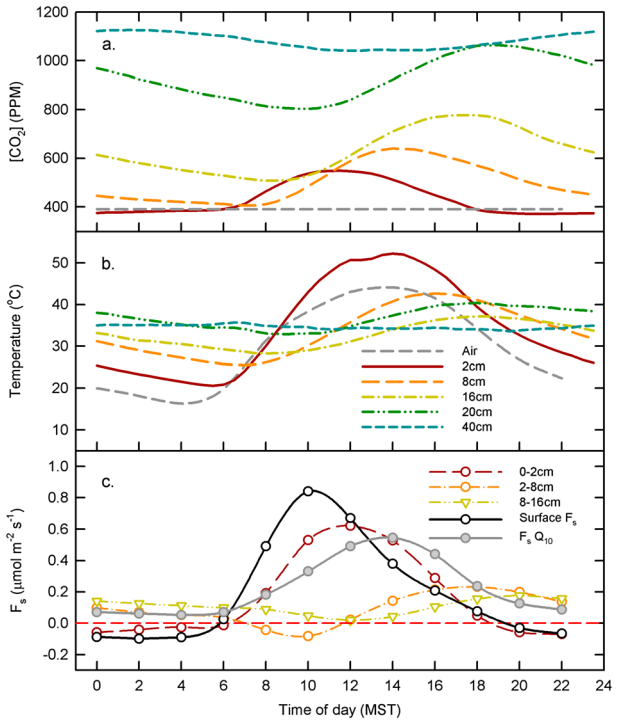

Figure 4. Diurnal dynamics of average (a) soil surface and subsurface CO_2 concentrations, (b) surface air and subsurface soil temperatures, and (c) soil chamber measured surface soil CO_2 efflux (F_s) and temperature-estimated F_s from a regression to determine Q_{10} ($F_s = a^* e^{(b^* T)}$ per *Bowling et al.* [2011]) and subsurface [CO_2] gradient-calculated subsurface F_s pooled across a 20 day period (DOY 155–175; 3–23 June).

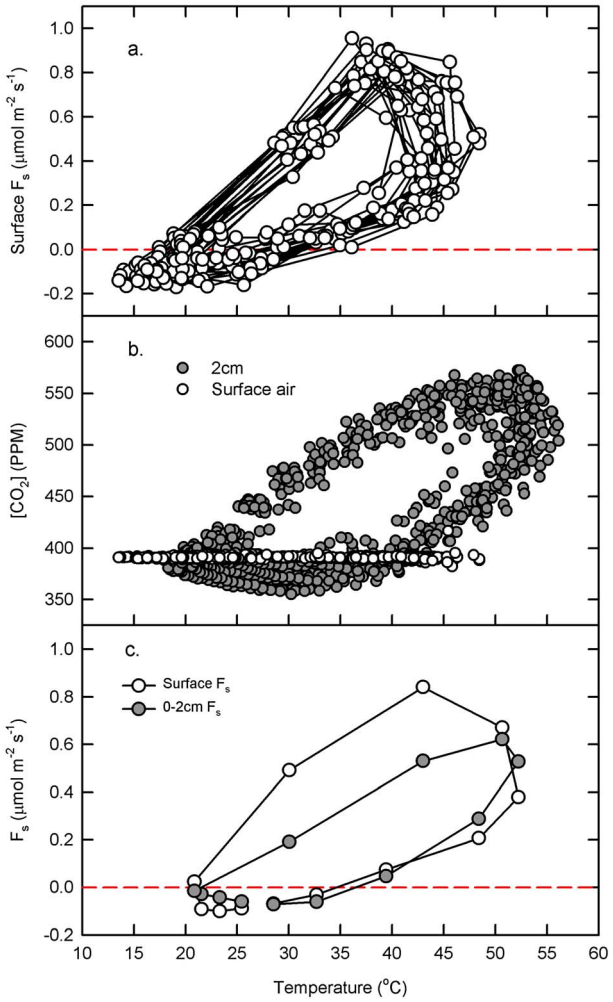

Figure 5. Temperature responses of (a) soil chamber measured soil surface CO_2 efflux (F_s), (b) soil CO_2 concentration at 2 cm depth and concurrent soil surface atmospheric [CO_2], and (c) average surface and 0–2 cm F_s responses to temperature at 2 cm for cross validation across a 20 day period (DOY 155–175; 3–23 June). Diurnal rotation is clockwise, with higher F_s and [CO_2] occurring from 06:00 to 10:00.

to undercanopy soils ($\chi^2 = 383.8$; $P \leq 0.001$; Figure 2). In undercanopy soils, the frequency of negative F_s exceeded positive values when air/soil temperature gradients were 11°C or greater (Figure 2a), as compared to 9°C in intercanopy (Figure 2b). Pooled across soil collars in both locations, F_s had a significant linear relationship with air/soil temperature gradients ($R^2 = 0.24$; $F_{1,734} = 229.34$; $P \leq 0.001$), with significant individual regressions for undercanopy ($F_{1,378} = 240.08$; $P \leq 0.001$; Figure 2c) and intercanopy locations ($F_{1,378} = 395.47$; $P \leq 0.001$; Figure 2d). Both regressions were anchored by negative F_s rates at stronger air/soil temperature gradients, with significantly different slopes and intercepts between undercanopy and intercanopy relationships ($F_{1,732} = 23.52$ and $F_{1,733} = 96.34$; $P \leq 0.001$, respectively). The steeper slope in undercanopy soil respiration collars (Figure 2c) was due to larger increases in undercanopy F_s following the few rains that occurred (Figure 1). These large after the rain F_s responses led to a markedly better goodness of fit using an exponential rather than a linear relationship for undercanopy soils ($F_s = 0.0009 + 0.9458 * e^{(0.66 * \Delta T)}$; $F_{2,377} = 294.08$; $P \leq 0.001$; Figure 2c). On nights where average nighttime F_s was negative in both locations, F_s was more negative in the intercanopy (-1.59 μmol m^{-2} s^{-1} ± 0.068 SE) compared to undercanopy rings (-0.91 μmol m^{-2} s^{-1} ± 0.069 SE; $F_{1,5} = 9.77$; $P = 0.026$).

[16] Volumetric soil moisture at 15 cm was consistently higher in intercanopy soils compared to undercanopy locations (Figure 3a); however, as undercanopy and intercanopy soils have identical particle size distributions (W. E. Emmerich, personal communication), the consistent difference between these through wetting and drying periods indicates that differences in $\theta_{15\ cm}$ were likely due to the influence of differences in soil bulk density on the soil moisture probe calibration equation [*Jacobsen and Schjønning* 1993]. It is likely that θ did not differ between locations in the dry periods. Pooled across all sampling dates, daily integrated F_s was lower in intercanopy locations ($F_{1,6} = 11.27$; $P = 0.015$) as well as nocturnally integrated F_s ($F_{1,6} = 15.31$; $P = 0.008$), with a significant location-by-time interaction for both parameters ($F_{91,546} = 12.87$; $P \leq 0.001$ for 24 h integrated and $F_{91,546} = 5.39$; $P \leq 0.01$ for nighttime integrated F_s, respectively). The two-way interaction due to much stronger positive diurnal and nighttime F_s responses to rain in the undercanopy soil collars as compared to intercanopy collars (Figures 3b and 3c). Lower diurnally integrated intercanopy F_s was also due to differences in nighttime F_s, as peak F_s (i.e., F_s averaged across 10:00 and 12:00 MST) did not differ between intercanopy (0.81 μmol m^{-2} s^{-1} ± 0.015 SE) and undercanopy soils (0.88 μmol m^{-2} s^{-1} ± 0.037 SE) pooled across the sampling period ($F_{1,6} = 2.38$; $P = 0.1741$; Figure 1). Peak F_s showed a significant location-by-DOY interaction ($F_{91,546} = 14.71$; $P \leq 0.01$) due to stronger after the rain peak F_s in undercanopy collars (Figure 1). Nighttime-integrated F_s was infrequently negative in undercanopy soil collars but was primarily negative in intercanopy soil collars (Figure 3c). This did not result in negative F_s integrated across 24 h in intercanopy soil collars (Figure 3b). Summed across the study period, intercanopy soils yielded 40.6% lower carbon yields (22.5 g C m^{-2} ± 1.31 SE) compared to those in undercanopy soils (32.9 g C m^{-2} ± 2.80 SE; one-way ANOVA $F_{1,6} = 11.27$; $P = 0.0153$). The total ecosystem-level F_s yield was estimated to be 23.5 g C over the entire study period (Figure 3d). By the end of the study, intercanopy nocturnal C accumulations were negative (-0.88 g C m^{-2} ± 0.351 SE) and significantly lower than undercanopy accumulations (5.4 g C m^{-2} ± 1.57 SE; one-way ANOVA $F_{1,6} = 15.31$; $P = 0.008$). Despite the occasional negative nightly integrated F_s in both locations and the overall negative C yield in intercanopy soils (Figure 3c), the total estimated nocturnal ecosystem-level F_s carbon yield was positive (0.59 g C m^{-2}; Figure 3d). Figure 4 presents diurnal dynamics averaged across a 20 day period, showing that soil surface and subsurface CO_2 concentrations (Figure 4a), temperature (Figure 4b) and surface and subsurface soil CO_2 flux (Figure 4c) in intercanopy soils when $\theta_{15\ cm}$ averaged 9.06%, and nocturnally integrated CO_2 were negative (DOY 155–175; average $F_s = -0.03$ g C m^{-2} night^{-1}; Figures 3a and 3c). Soil CO_2 uptake was associated with clear [CO_2] concentration gradients from 40 to 2 cm and [CO_2] at 2 cm lower than concentrations at the soil surface (Figure 4a). Initiation of morning soil surface efflux preceded changes in [CO_2] at 2 cm, which, in

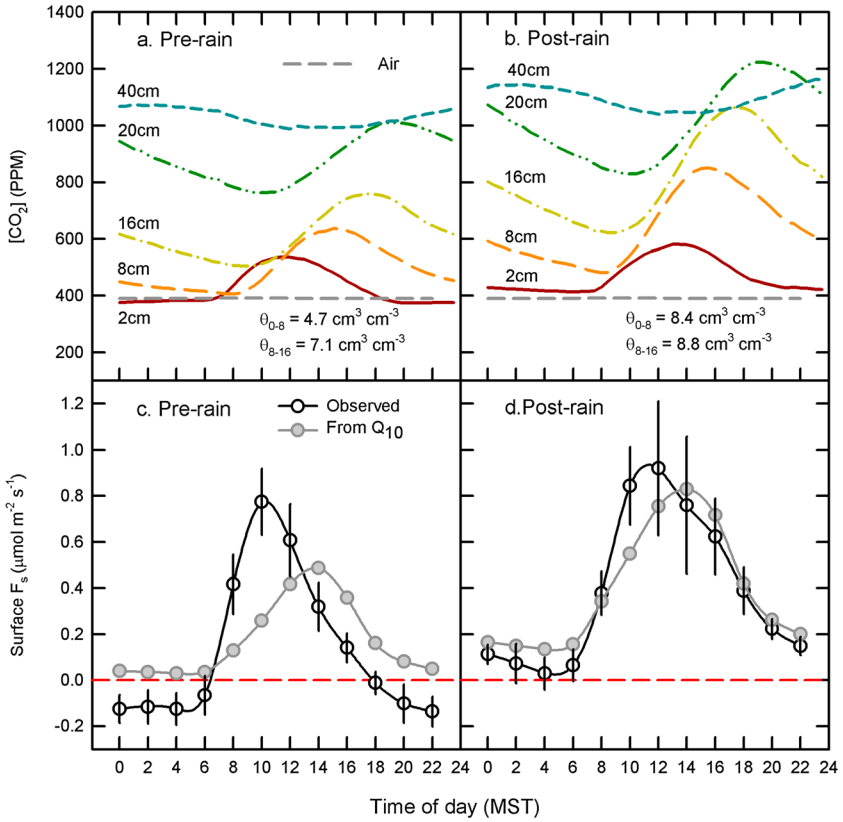

Figure 6. Diurnal dynamics of soil surface atmospheric and subsurface $[CO_2]$ averaged over the 7 day (a) pre-rain (DOY 122–128; 1–7 May) and (b) post-rain (DOY 132–138; 11–17 May) periods. Soil-chamber measured soil surface CO_2 efflux (F_s) and temperature-estimated F_s from a regression to determine Q_{10} ($F_s = a^* e^{(b^* T)}$ per *Bowling et al.* [2011]) for (c) pre-rain and (d) post-rain periods. Bars are ±1 standard deviation.

turn, increased sooner and more strongly than $[CO_2]$ at 8 and 16 cm and even exceeded concentrations at 8 cm through much of the morning (Figure 4a). This resulted in a morning period where CO_2 flux at 2 cm was bidirectional, with upward efflux toward the soil surface (i.e., positive F_s at 0–2 cm) and downward into the soil profile (i.e., negative F_s at 2–8 cm; Figure 4c). Soil surface F_s peaked at 10:00 MST, well before 2 cm $[CO_2]$ (Figure 4a) and F_s 0–2 cm did (Figure 4c); more frequent surface F_s sampling may have shown that peak efflux rates were associated with the transient period with essentially no soil $[CO_2]$ gradient between 16 and 2 cm and an overall $[CO_2]$ of 545–560 ppm (Figure 4a). Afternoon declines in surface F_s and F_s at 0–2 cm and 2–8 cm were associated with reestablishment of clear $[CO_2]$ gradients from 40 to 2 cm that started after $[CO_2]$ at 2 cm declined to levels below those at 8 and 16 cm (Figure 4a). Rises and declines in surface F_s and $[CO_2]$, and therefore subsurface F_s, were temporally offset from their associated temperatures (Figure 4b). Compared to surface F_s predicted from surface air temperature ($F_s = ae^{(b^* T\text{air})}$, which gave a Q_{10} of 1.01) [*Bowling et al.*, 2011], observed surface F_s showed markedly greater morning increases than would be predicted from T_{air}, and F_s estimated from T_{air} also did not predict nighttime soil CO_2 uptake (Figure 4d). Temperature-derived daily integrated F_s was 0.019 g C m^{-2} d^{-1} compared to 0.017 g C m^{-2} d^{-1} for observed efflux rates, a 9.3% overestimation.

[17] Stronger positive morning surface F_s and higher $[CO_2]$ resulted in distinct diurnal temperature hysteresis (Figure 5a), as did $[CO_2]$ at 2 cm soil depths (Figure 5b). Across most soil temperatures, 0–2 cm profile estimated flux and surface F_s were in good agreement, varying from approximately −0.03 to +0.06 μmol m^{-2} s^{-1}; however, profile-estimated F_s underestimated the 08:00 and 10:00 F_s by approximately 0.3 μmol m^{-2} s^{-1} (Figure 5c). Integrating under the pooled daily curves for surface and 0–2 cm profile F_s (Figure 4), the underestimation by profile-estimated F_s in the morning led to a 16% underestimation of daily integrated surface CO_2 flux (0.0144 g C m^{-2} d^{-1} compared to 0.0172 g C m^{-2} d^{-1}).

[18] Figure 6 summarizes diurnal surface F_s and subsurface $[CO_2]$ and temperatures for two 7 day periods: one (DOY 122–128) when shallow soils were dry and showed distinct vertical distribution in θ (Figure 6a) with a negative nocturnal integrated surface F_s (−0.05 g C m^{-2} $night^{-1}$; Figure 3c), and the other (DOY 132–138), after a 9.4 mm rain, over a period of higher and more even depth distribution of θ (Figure 6b) and positive nocturnal F_s (0.05 g C m^{-2} $night^{-1}$; Figure 3c). Over the pre-rain period, F_s (Figure 6a) and subsurface $[CO_2]$ dynamics (Figure 6c) were nearly identical to those observed later over a 20 day premonsoon period (DOY 155–175; Figure 4a). Over the post-rain period, the concentrations of the entire profile went up despite shallow infiltration depths somewhere between 5 and 15 cm

(data not shown). While the soil CO_2 concentration gradient between 20 and 2 cm remained consistent throughout the 24 h diurnal cycle (Figure 6b), soil CO_2 efflux more closely followed soil surface air temperatures compared to when it was dry (Figure 6d). Interestingly, the Q_{10} estimated for the post-rain period did not differ from that calculated under dry conditions (1.01). Unlike under drier soil conditions, CO_2 at 20 cm exceeded 40 cm levels through much of the night (Figure 6b). The overall daily integrated F_s for the pre-rain period was 0.012 g C m^{-2} d^{-1} using observed rates and 0.015 g C m^{-2} d^{-1} using temperature-estimated F_s, an 18.7% overestimation, compared to 0.319 g C m^{-2} d^{-1} and 0.324 g m^{-2} d^{-1} for observed and temperature-estimated F_s over the 7 day post-rain period, respectively.

4. Discussion

[19] Negative soil CO_2 efflux occurred frequently throughout the three-month premonsoon study period, especially in intercanopy soils (Figure 1), and was of sufficient strength and duration to result in negative nighttime integrated F_s, especially in intercanopy locations (Figure 3c). At no point was soil carbon uptake observed under daytime conditions (Figure 1), so it is unlikely that photosynthetic activity by the soil cryptobiotic community drove soil CO_2 uptake, as observed in other arid land systems [*Bowling et al*., 2011]. As in other studies documenting negative F_s [*Parsons et al*., 2004; *Ball et al*., 2009; *Xie et al*., 2009], nocturnal soil surface CO_2 uptake coincided with strong soil-air temperature gradients (Figure 2), counter to those showing that nocturnal CO_2 outgassing is favored under strong soil-air temperature gradients [*Weisbrod et al*., 2009] and effects on soil air buoyancy that result from thermal gradient effects on CO_2 partial pressures [*Kowalski and Sánchez-Cañete*, 2010; *Sánchez-Cañete et al*., 2013b]. However, these studies examined exchange through systems underlain by karst geology, or in systems with connections to large caves, features not present in the coarse-textured, sandy loam soils at the Lucky Hills site [*Breckenfeld*, 2008]. The frequency distribution and magnitude of negative F_s were not the same between undercanopy and intercanopy locations (Figure 2), as hypothesized. Arid land shrubs serve as accumulation points for soil and anything in it, including inorganic carbon [*Titus et al*., 2002; *Emmerich*, 2003], which is physically displaced quickly by infiltration following isolated rains, and can affect postpulse ecosystem carbon balance [*Huxman et al*., 2004]. Though dry conditions curtail activity of soil microbes and plant roots [*Cable et al*., 2008], biotic activity is still likely to be greater under plant canopies [*Barron-Gafford et al*., 2011]. These two features would explain why undercanopy soils responded more strongly to rain (Figure 1). In addition, reduction of incident solar radiation in the undercanopy during the day may have lowered the depth and degree of undercanopy soil warming [*D'Odorico et al*., 2010], which likely reduced the frequency of nocturnal soil CO_2 uptake (Figure 2) [see also *Ball et al*., 2009; *Xie et al*., 2009]. Overall, our findings indicate that even when surface F_s is negative across seasonal dry periods, it is a net flux, reflecting both positive and negative contributions of biotic and abiotic carbon processes.

[20] The instantaneous rates of nighttime soil CO_2 uptake at the Lucky Hills site were similar to those observed in Antarctic Dry Valley ecosystems [*Parsons et al*., 2004; *Ball et al*., 2009] and hyper-alkali soils in central Asia deserts [*Xie et al*., 2009]. More frequent and stronger nocturnal soil CO_2 uptake contributed to lower total soil C yields in intercanopy soils (Figure 3b), as peak daytime soil efflux rates did not differ between intercanopy and undercanopy soils when conditions were dry (Figure 1). The strong undercanopy F_s responses to the few isolated rains that occurred (Figure 1) led to disproportionate contributions from these soils to ecosystem-level F_s, as evidenced by positive nocturnal ecosystem F_s carbon yields summed across the study period (0.59 g C m^{-2}; Figure 3c), despite intercanopy soils taking up −0.5 to −1.2 g C m^{-2} (Figure 3b), supporting our hypothesis. In addition to highlighting the importance of water in arid land soil CO_2 exchange, these results show that plant canopy modulation of soil respiratory dynamics when water is available [*Cable et al*., 2008, 2011; *Barron-Gafford et al*., 2011] extends to soil carbon processes over prolonged seasonal dry periods as well. Our results also suggest that nocturnal soil CO_2 uptake may not be as major a feature in global carbon cycles as some have conjectured [*Xie et al*., 2009]. However, at an unvegetated Great Basin desert playa in Nevada, *Yates et al*. [2013] demonstrated that soil CO_2 uptake drove the nocturnal atmospheric mixing ratio to levels of 340–380 ppm, well below average background [CO_2]. At no point in our study was such a decrease in atmospheric [CO_2] noted, either at the soil surface (Figures 4a and 5b) or in [CO_2] measured on the EC tower (data not shown). In addition, at a desert grassland site with high soil carbonates [*Emmerich*, 2003], but much higher plant cover located 10.5 km east from the Lucky Hills site, premonsoon negative nocturnal F_s was never observed [*Hamerlynck et al*., 2013]. These findings and ours show that in addition to variation in soil carbonate concentrations, plant cover modulates the processes underlying abiotic soil CO_2 dynamics in arid lands.

[21] The temporal trends of our data support the ventilation-driven carbonate deposition/dissolution mechanism proposed by *Roland et al*. [2013]. On nights with soil CO_2 uptake, soil [CO_2] at 2 cm was below atmospheric levels, and there was a clear upward [CO_2] gradient toward 2 cm, resulting in a convergence of F_s toward 2 cm, especially from 22:00 to 06:00, when negative surface efflux was most pronounced (Figures 4 and 6a). This flux convergence indicates CO_2 consumption at 2 cm, consistent with *Roland et al*.'s [2013] model of sustained nocturnal carbonate dissolution serving as a soil CO_2 sink for atmospheric and deeper soil CO_2. *Roland et al*. [2013] conjectured upward diffusion of CO_2 from deep within the soil, in their case, from cracks and caves in their karstic system, induced $CaCO_3$ dissolution at shallower depths, driving nocturnal soil CO_2 uptake. The Lucky Hills site is not in a karst setting that allows for higher soil air exchange rates and a greater volume of soil involved in soil gas exchange at the surface. Soil cooling at night under dry conditions is associated with upward migration and, sometimes, deposition of water vapor onto soil particles and rock clasts [*Nobel and Geller*, 1987; *Scanlon*, 1994; *Berndtsson et al*., 1996]. It may be that changes in soil water vapor concentration led to sustained $CaCO_3$ dissolution and absorption of CO_2 near the soil surface (Figures 4a and 6a), as required by *Roland et al*.'s [2013] model. It is unlikely that condensation and deposition were part of the process at our site, as prevailing soil and air temperatures never resulted in dew fall conditions over the course of the study period

(data not shown). In the morning, surface F_s increased before rises in [CO_2] at 2 cm, which were followed sequentially by rises in [CO_2] at 8, 16, and 20 cm (Figures 4a and 6a). This might reflect surface and air warming (Figure 4b), inducing convective exchange sufficient to drive outgassing and carbonate precipitation [*Roland et al*., 2013; *Yates et al*., 2013]. Over the morning, [CO_2] at 2 cm were greater than atmospheric levels and [CO_2] at 8 cm (Figures 4a and 6a), resulting in a flux divergence in F_s at 2 cm, with upward, positive flux from 2 cm to the soil surface, and downward, negative flux toward 8 cm (Figure 4c). We believe that this bidirectional F_s is likely to be ventilation-induced carbonate precipitation, with soil around 2 cm depth acting as a CO_2 source following nighttime carbonate dissolution and HCO_3 accumulation [*Roland et al*., 2013; *Yates et al*., 2013].

[22] Under dry conditions, afternoon declines in surface F_s were more pronounced than when wet (Figures 4 and 6). This might be a consequence of CO_2 concentrations at 8 cm initially being below levels at 2 and 16 cm, which could reduce the overall soil volume involved in outgassing. Or, it may simply be that the overall lower CO_2 concentration under drier soil conditions (Figures 6a and 6b) leads to more rapid depletion of soil CO_2. Unlike *Rey et al*. [2012] or *Roland et al*. [2013], daytime CO_2 outgassing at our site was not closely associated with increasing u^* (data not shown). The turbulence dependence of these ecosystem CO_2 fluxes was due to extensive soil-atmosphere connections, either via karst [*Roland et al*., 2013] or deep, fluid geothermal sources [*Rey et al*., 2012], neither of which are present at the Lucky Hills site. It may be that the much smaller soil gas exchange rates and, hence, volumes at our site likely reduced the amount of daytime outgassing such that by afternoon, surface F_s decreased even as u^* remained high through the afternoon. When soils were wetter, the upward nighttime [CO_2] gradient below 2 cm did not always extend to 40 cm, which could limit the soil volume involved $CaCO_3$ dissolution and nocturnal soil uptake (Figure 6b). Also, overall soil [CO_2] was higher when the soil was wet, and the [CO_2] gradient from 2 to 20 cm was in place throughout the diurnal cycle (Figure 6b). This would facilitate sustained nocturnal soil surface CO_2 efflux, as well as supported higher afternoon F_s (Figure 6d).

[23] The distinct temperature hysteresis apparent in surface F_s (Figure 5a) was stronger than surface fluxes estimated for 0–2cm (Figure 5c), even though the latter included the strong temperature hysteresis apparent in [CO_2] at 2 cm (Figure 5b). Surface F_s also showed stronger morning temperature responses than would be expected from using the standard and commonly used Q_{10} exponential temperature model (Figure 4a). These F_s-temperature hysteresis responses may be also due to eddy-assisted convective exchange as the soil warms. Alternatively, temperature hysteresis may reflect differences in the temperature kinetics of carbonate precipitation and dissolution [*Cerling*, 1984; *Breecker et al*., 2009] to morning increases and afternoon declines in [CO_2] and F_s. The relative contributions of these distinct processes to changes in soil [CO_2] dynamics cannot be readily ascertained from our data. Respiratory temperature hysteresis in arid land systems has been explained as resulting from diurnal changes in assimilate transport stimulating root activity and root exudates enhancing microbial activity [*Barron-Gafford et al*., 2011]. In addition, soil modeling efforts have shown that surface hysteresis responses can be induced by distinct temporal dynamics of subsurface physical transport processes alone [*Phillips et al*., 2011]. However, in studies relying on biologically derived respiration signals, diurnal temperature hysteresis runs counterclockwise, with greater F_s yields at similar afternoon temperatures [*Phillips et al*., 2011; *Barron-Gafford et al*., 2011]. In contrast, our results run clockwise, with higher morning rates and lower afternoon and evening rates at similar temperatures (Figure 5). These results suggest that accounting for changes in the diurnal trajectories of F_s temperature responses could be used to better model and predict soil carbon dynamics in arid land systems. Though total F_s fluxes are low, dry periods in arid land systems can prevail over the bulk of the year, and, in some systems, can persist over years [*Sheppard et al*., 2002; *Houston and Hartley*, 2003; *Parsons et al*., 2004]. Our results showed temperature-derived estimates of F_s overestimated diurnal F_s carbon yields by approximately 9% (Figure 4a) to 19% (Figure 6c) when soils were drier, but were in close agreement over the short period following rainfall sufficient to raise soil moisture content (Figure 6d). Future modeling of arid land carbon cycling should account for shifts in the dominance of organic and inorganic carbon dynamics in ecosystem fluxes [*Kowalski et al*., 2008; *Serrano-Ortiz et al*., 2010] and, furthermore, should also account for the strong temperature hysteresis apparent in abiotic carbon fluxes in water-limited systems.

[24] In summary, our results clearly show that nocturnal soil CO_2 uptake originates from near, or even at, the soil surface, in soils with high soil inorganic carbon content [*Emmerich*, 2003; *Breckenfeld*, 2008; *Yates et al*., 2013]. Regularly recurring prolonged dry periods in southwest U.S. arid lands represent a baseline carbon source, whose losses must be offset by C uptake activity during seasonal rainy periods, which is modulated by the seasonal distribution of rainfall [*Scott et al*., 2010; *Hamerlynck et al*., 2013]. Climate models predict lower cool season rainfall and warmer cool season temperatures, in addition to greater variation in monsoon season precipitation [*Seager et al*., 2007; *McAfee and Russell*, 2008]. Such conditions are likely to increase the duration and intensity of premonsoon drought. This could enhance nocturnal soil CO_2 uptake, shifting the diurnal balance of carbonate dissolution/precipitation, and thereby the baseline dry season carbon loss that subsequent monsoon season plant activity would have to offset. Elevated carbon dioxide may also have a strong direct effect on these abiotic carbon processes over these dry periods. An important driver of nocturnal CO_2 uptake is the difference in CO_2 concentration between the atmosphere and 2 cm (Figures 4 and 6). Even if changes in temperature and precipitation do not dramatically affect soil [CO_2] and temperature dynamics, increasing atmospheric CO_2 will increase the probability of nighttime carbonate dissolution. This could eventually lead to a spatial shift to more undercanopy nocturnal carbonate dissolution and soil uptake. Thus, rising atmospheric CO_2 has the potential to alter the spatial and temporal distributions of pedogenic carbonate formation over warm dry periods [*Breecker et al*., 2009]. This would represent a greater direct ecosystem-level response to elevated carbon dioxide, given the lack of elevated carbon dioxide concentration effects on long-term soil water and plant-mediated carbon sequestration in desert ecosystems [*Nowak et al*., 2004; *Newingham et al*., 2013].

[25] **Acknowledgments.** The authors thank Michelle Cavanaugh for her invaluable field assistance. This paper is the result of a fellowship funded by the OECD Cooperative Research Program: Biological Resource Management for Sustainable Agricultural Systems to R. L. Scott. Travel for E. P. Sánchez-Cañete was supported by the Andalusian regional government project GECARBO (P08-RNM-3721). USDA is an equal opportunity employer.

References

Ball, B. A., R. A. Virginia, J. E. Barrett, A. N. Parsons, and D. H. Wall (2009), Interactions between physical and biotic factors influence CO_2 flux in Antarctic dry valley soils, *Soil Biol. Biochem.*, *41*, 1510–1517.

Barron-Gafford, G. A., R. L. Scott, G. D. Jenerette, and T. E. Huxman (2011), The relative controls of temperature, soil moisture, and plant functional group on soil CO_2 efflux at diurnal, seasonal, and annual scales, *J. Geophys. Res.*, *116*, G01023, doi:10.1029/2011JG001442.

Barron-Gafford, G. A., R. L. Scott, G. D. Jenerette, E. P. Hamerlynck, and T. E. Huxman (2012), Temperature and precipitation controls over leaf- and ecosystem-level CO_2 flux along a woody plant encroachment gradient, *Global Change Biol.*, *18*, 1389–1400, doi:10.1111/j.1365-2486.2011.02599.x.

Berndtsson, R., K. Nodomi, H. Yasuda, T. Persson, H. Chen, and K. Jinno (1996), Soil water and temperature patterns in an arid desert sand dune, *J. Hydrol.*, *185*, 221–240.

Bhark, E. W., and E. E. Small (2003), Association between plant canopies and the spatial patterns of infiltration in shrubland and grassland of the Chihuahuan Desert, New Mexico, *Ecosystems*, *6*, 185–196, doi:10.1007/s10021-002-0210-9.

Bird, R. B., W. E. Stewart, and E. N. Lightfoot (2002), *Transport Phenomena*, John Wiley, Cambridge.

Bowling, D. R., E. E. Grote, and J. J. Belnap (2011), Rain pulse responses of soil CO_2 exchange by biological soil crusts and grasslands of the semiarid Colorado Plateau, United States, *J. Geophys. Res.*, *116*, G03028, doi:10.1029/2011JG001643

Breckenfeld, D. J. (2008), Soil survey of Walnut Gulch Experimental Watershed. A special report, U.S. Dep. of Agric., Soil Conservation Service, 312 pp.

Breecker, D. O., Z. D. Sharp, and L. D. McFadden (2009), Seasonal bias in the formation and stable isotopic composition of pedogenic carbonate in modern soils from central New Mexico, USA, *Geol. Soc. Am. Bull.*, *121*, 630–640, doi:10.1130/B26413.1.

Breshears, D. D., et al. (2005), Regional vegetation die-off in response to global-change-type drought, *Proc. Natl. Acad. Sci. U.S.A.*, *102*, 15,144–15,148, doi:10.1073/pnas.0505734102.

Cable, J. M., K. Ogle, D. G. Williams, J. F. Weltzin, and T. E. Huxman (2008), Soil texture drives response of soil respiration to precipitation pulses in the Sonoran Desert: Implications for climate change, *Ecosystems*, *11*, 961–979, doi:10.1007/s10021-008-9172-x.

Cable, J. M., et al. (2011), The temperature response of soil respiration in deserts: A seven desert synthesis, *Biogeochemistry*, *103*, 71–90, doi:10.1007/s10533-010-9448-z.

Caldwell, T. G., M. H. Young, J. Zhu, and E. V. McDonald (2008), Spatial structure of hydraulic properties from canopy to interspace in the Mojave Desert, *Geophys. Res. Lett.*, *35*, L19406, doi:10.1029/2008GL035095.

Cerling, T. E. (1984), The stable isotopic composition of modern soil carbonate and its relationship to climate, *Earth Planet. Sci. Lett.*, *71*, 229–240.

D'Odorico, P., K. Caylor, G. S. Okin, and T. M. Scanlon (2007), On soil moisture-vegetation feedbacks and their possible effects on the dynamics of dryland ecosystems, *J. Geophys. Res.*, *112*, G04010, doi:10.1029/2006JG000379.

D'Odorico, P., J. D. Fuentes, W. T. Pockman, S. L. Collins, Y. He, J. S. Medeiros, S. DeWekker, and M. E. Litvak (2010), Positive feedback between microclimate and shrub encroachment in the northern Chihuahuan desert, *Ecosphere*, *1*, art 17, doi:10.1890/ES10-0073.1.

Duniway, M. C., K. A. Synder, and J. E. Herrick (2010), Spatial and temporal patterns of water availability in a grass-shrub ecotone and implications for grassland recovery in arid environments, *Ecohydrology*, *3*, 55–67, doi:10.1002/eco.94.

Emmerich, W. E. (2003), Carbon dioxide fluxes in a semiarid environment with high carbonate soils, *Agric. For. Meteorol.*, *116*, 91–102.

Fernandez, D. P., J. C. Neff, J. Belnap, and R. L. Reynolds (2006), Soil respiration in the cold desert environment of the Colorado Plateau (USA): Abiotic regulators and thresholds, *Biogeochemistry*, *78*, 247–265, doi:10.1007/s10533-005-4278-0.

Goodrich, D. C., T. O. Keefer, C. L. Unkrich, M. H. Nichols, H. B. Osborn, J. J. Stone, and J. R. Smith (2008), Long-term precipitation database, Walnut Gulch Experimental Watershed, Arizona, United States, *Water Resour. Res.*, *44*, W05S04, doi:10.1029/2006WR005782.

Hamerlynck, E. P., R. L. Scott, and G. A. Barron-Gafford (2013), Consequences of cool-season drought-induced plant mortality to Chihuahuan Desert grassland ecosystem and soil respiration dynamics, *Ecosystems*, *16*, 1178–1191, doi:10.1007/s10021-13-9675-y.

Houston, J., and A. J. Hartley (2003), The central Andean west-slope rainshadow and its potential contribution to the origin of hyper-aridity in the Atacama Desert, *Int. J. Climatol.*, *23*, 1453–1646, doi:10.1002/joc.938.

Huxman, T. E., J. M. Cable, D. D. Ignace, J. A. Eilts, N. B. English, J. Weltzin, and D. G. Williams (2004), Response of net ecosystem gas exchange to a simulated precipitation pulse in a semi-arid grassland: The role of native versus non-native grasses and soil texture, *Oecologia*, *141*, 295–305, doi:10.1007/s.00442-03-1389-y.

Jacobsen, O. H., and P. Schjønning (1993), A laboratory calibration of time domain reflectometry for soil water measurement including effects of bulk density and texture, *J. Hydrol.*, *151*, 147–157.

Jenerette, G. D., R. L. Scott, and T. E. Huxman (2008), Whole ecosystem metabolic pulses following precipitation pulses, *Funct. Ecol.*, *22*, 924–930, doi:10.1111/j.1365-2435.2008.01450.x.

Jones, H. G. (1992), *Plants and Microclimate: A Quantitative Approach to Environmental Plant Physiology*, pp. 51, Cambridge Univ. Press, New York.

Keefer, T. O., M. S. Moran, and G. B. Paige (2008), Long-term meteorological and soil hydrology database, Walnut Gulch Experimental Watershed, Arizona, United States, *Water Resour. Res.*, *44*, W05S07, doi:10.1029/2006WR005702.

Kowalski, A., and D. Argüeso (2011), Scalar arguments of the mathematical functions defining molecular and turbulent transport of heat and mass in compressible fluids, *Tellus, Ser. B*, *63*, 1059–1066, doi:10.1111/j.1600-0889.2011.00579.x.

Kowalski, A. S., and E. P. Sánchez-Cañete (2010), A new definition of the virtual temperature, valid for the atmosphere and the CO_2-rich air of the vadose zone, *J. Appl. Meteorol. Climatol.*, *49*, 1692–1695, doi:10.1175/2010JAMC2534.1.

Kowalski, A. S., P. Serrano-Ortiz, I. A. Janssens, S. Sanchez-Moral, S. Cuezva, F. Domingo, A. Were, and A. Alados-Arboledas (2008), Can flux tower research neglect geochemical CO_2 exchange, *Agric. For. Meteorol.*, *148*, 1045–1054, doi:10.1016/j.agformet.2008.02.004.

Loik, M. E., D. D. Breshears, W. K. Lauenroth, and J. Belnap (2004), A multi-scale perspective of water pulses in dryland ecosystems: Climatology and ecohydrology of the western USA, *Oecologia*, *141*, 129–281, doi:10.1007/s0042-004-1570-y.

McAfee, S. A. and J. L. Russell (2008), Northern Annular Mode impact on spring climate in the western United States, *Geophys. Res. Lett.*, *35*, L17701, doi:10.1029/2008GL034828.

McAuliffe, J. R., and E. P. Hamerlynck (2010), Perennial plant mortality in the Sonoran and Mojave deserts in response to severe, multi-year drought, *J. Arid Environ.*, *74*, 885–896, doi:10.1016/j.aridenv.2010.01.001.

Miriti, M. N., S. Rodriguez-Buritica, S. J. Wright, and H. F. Howe (2007), Episodic death across species of desert shrubs, *Ecology*, *88*, 23–36.

Moldrup, P., T. Olesen, J. Gamst, P. Schjønning, T. Yamaguchi, and D. E. Rolston (2000), Predicting the gas diffusion coefficient in repacked soil: Water-induced linear reduction model, *Soil Sci. Soc. Am. J.*, *64*, 1588–1594.

Newingham, B. A., C. H. Vanier, T. N. Charlet, K. Ogle, S. D. Smith, and R. S. Nowak (2013), No cumulative effect of 10 years of elevated [CO_2] on perennial plant biomass components in the Mojave Desert, *Global Change Biol.*, *19*, 2168–2181, doi:10.1111/gcb.12177.

Nobel, P. S., and G. N. Geller (1987), Temperature modeling of wet and dry desert soils, *J. Ecol.*, *75*, 247–258.

Nowak, R. S., S. F. Zitzer, D. Babcock, V. Smith-Longozo, T. N. Charlet, J. S. Coleman, J. R. Seemann, and S. D. Smith (2004), Elevated atmospheric CO_2 does not conserve soil water in the Mojave Desert, *Ecology*, *85*, 93–99.

Parsons, A. N., J. E. Barrett, D. H. Wall, and R. A. Virginia (2004), Soil carbon dioxide flux in Antarctic dry valley ecosystems, *Ecosystems*, *7*, 286–295, doi:10.1007/s10021-003-0132-1.

Pennington, D. D., and S. L. Collins (2007), Response of aridland ecosystem to interannual climate variability and prolonged drought, *Landscape Ecol.*, *22*, 897–910, doi:10.1007/s10980-006-9071-5.

Phillips, C. L., N. Nickerson, D. Risk, and B. J. Bond (2011), Interpreting diel hysteresis between soil respiration and temperature, *Global Change Biol.*, *17*, 515–527, doi:10.1111/j.1365-2486.2010.02250.x.

Plestenjak, G., K. Eler, D. Vodnik, M. Ferlan, M. Čater, T. Kanduč, P. Simončič, and N. Ogrinc (2012), Sources of soil CO_2 in calcareous grassland with woody plant encroachment, *J. Soils Sediments*, *12*, 1327–1338, doi:10.1007/s11368-012-0564-3.

Pockman, W. T., and E. E. Small (2010), The influence of spatial patterns of soil moisture on the grass and shrub responses to a summer rainstorm in a Chihuahuan Desert ecotone, *Ecosystems*, *13*, 511–525, doi:10.1007/s10021-010-9337-2.

Potts, D. L., T. E. Huxman, J. M. Cable, N. B. English, D. D. Ignace, J. A. Eilts, M. J. Mason, J. F. Weltzin, and D. G. Williams (2006), Antecedent moisture and seasonal precipitation influence the response of canopy-scale carbon and water exchange to rainfall pulses in a semi-arid grassland, *New Phytol.*, *170*, 849–860, doi:10.1111/j.1469-8137.2006.01732.x.

Renard, K. G., M. H. Nichols, D. A. Woolhiser, and H. B. Osborn (2008), A brief background on the U.S. Department of Agriculture, Agriculture Research Service Walnut Gulch Experimental Watershed, *Water Resour. Res.*, *44*, W05S02, doi:10.1029/2006WR005691.

Rey, A., L. Belelli-Marchesini, A. Were, P. Serrano-Ortiz, G. Etiope, D. Papale, F. Domingo, and E. Pegoraro (2012), Wind as a main driver of the net ecosystem carbon balance of a semiarid Mediterranean steppe in the South East of Spain, *Global Change Biol.*, *18*, 539–554, doi:10.1111/j.1365-2486.2011.02534.x.

Roland, M., et al. (2013), Atmospheric turbulence triggers pronounced diel pattern in karst carbonate geochemistry, *Biogeosci. Discuss.*, *10*, 5009–5017, doi:10.5194/bg-10-5009-2013.

Sánchez-Cañete, E. P., A. S. Kowalski, P. Serrano-Ortiz, O. Pérez-Priego, and F. Domingo (2013a), Deep CO_2 soil inhalation/exhalation induced by synoptic pressure changes and atmospheric tides in a carbonated semiarid steppe, *Biogeosciences*, *10*, 6591–6600, doi:10.5194/bg-10-6591-2013.

Sánchez-Cañete, E. P., P. Serrano-Ortiz, F. Domingo, and A. S. Kowalski (2013b), Cave ventilation is influenced by variations in the CO_2-dependent virtual temperature, *Int. J. Speleol.*, *42*, 1–8, doi:10.5038/1827-806X.42.1.1.

Scanlon, B. R. (1994), Water and heat fluxes in desert soils: 1. Field studies, *Water Resour. Res.*, *30*, 709–719.

Scholes, R. J., and S. R. Archer (1997), Tree-grass interactions in savannas, *Annu. Rev. Ecol. Syst.*, *28*, 517–544.

Scott, R. L., W. L. Cable, and K. R. Hultine (2008), The ecohydrologic significance of hydraulic redistribution in a semiarid savanna, *Water Resour. Res.*, *44*, W02440, doi:10.1029/2007WR006149.

Scott, R. L., E. P. Hamerlynck, G. D. Jenerette, M. S. Moran, and G. A. Barron-Gafford (2010), Carbon dioxide exchange in a semidesert grassland through drought-induced vegetation change, *J. Geophys. Res.*, *115*, G03026, doi:10.1029/2010JG001348.

Seager, R., et al. (2007), Model predictions of an imminent transition to a more arid climate in Southwestern North America, *Science*, *316*, 1181–1184, doi:10.1126/science.1139601.

Serrano-Ortiz, P., M. Roland, S. Sanchez-Moral, I. A. Janssens, F. Domingo, Y. Godderis, and K. S. Kowalski (2010), Hidden, abiotic CO_2 flows and gaseous reservoirs in the terrestrial carbon cycle: Review and perspectives, *Agric. For. Meteorol.*, *150*, 321–329, doi:10.1016/j.agformet.2010.01.002.

Sheppard, P. R., A. C. Comrie, G. D. Packin, K. Angersbach, and M. K. Huges (2002), The climate of the US Southwest, *Clim. Res.*, *21*, 219–238.

Skirvin, S., M. Kidwell, S. Bidenbender, J. P. Henley, D. King, C. H. Collins, M. S. Moran, and M. Weltz (2008), Vegetation data, Walnut Gulch Experimental Watershed, Arizona, United States, *Water Resour. Res.*, *44*, W05S08, doi:10.1029/2006WR005724.

Tang, J. W., D. D. Baldocchi, and L. K. Xu (2003), Assessing soil CO_2 efflux using continuous measurements of CO_2 profiles in soils with small solid-state sensors, *Agric. For. Meteorol.*, *118*, 207–220, doi:10.1016/S0168-1923(03)00112-6.

Titus, J. H., R. S. Nowak, and S. D. Smith (2002), Soil resource heterogeneity in the Mojave Desert, *J. Arid Environ.*, *52*, 269–292, doi:10.1006/jare.2002.1010.

Weisbrod, N., M. I. Dragila, U. Nachson, and M. Pillersdorf (2009), Falling through the cracks: The role of fractures in Earth-atmosphere gas exchange, *Geophys. Res. Lett.*, *36*, L02401, doi:10.1029/2008GL036096.

Williams, K., M. M. Caldwell, and J. J. Richards (1993), The influence of shade and clouds on soil water potential, the buffered behavior of hydraulic lift, *Plant Soil*, *157*, 83–95.

Xie, J., Y. Li, C. Zhai, C. Li, and Z. Lan (2009), CO_2 adsorption by alkaline soils and its implication to the global carbon cycle, *Environ. Geol.*, *56*, 953–961, doi:10.1007/s00254-008-1197-0.

Yates, E. L., A. M. Detweiler, L. T. Iraci, B. M. Bebout, C. P. McKay, K. Schiro, E. J. Sheffner, C. A. Kelley, J. M. Tadić, and M. Lowenstein (2013), Assessing the role of alkaline soils on the carbon cycle at a playa site, *Environ. Earth Sci.*, *70*, 1047–1056, doi:10.1007/s12665-012-2194-x.